

AD-A174 127

12

AD

TECHNICAL REPORT ARCCB-TR-86034

# ACOUSTOELASTIC EFFECTS IN AUTOFRETTAGED STEEL CYLINDERS

W. SCHOLZ

J. FRANKEL

OCTOBER 1986

DTIC  
ELECTE  
NOV 19 1986  
S D  
A



US ARMY ARMAMENT RESEARCH AND DEVELOPMENT CENTER  
CLOSE COMBAT ARMAMENTS CENTER  
BENET WEAPONS LABORATORY  
WATERVLIET, N.Y. 12189-4050

DTIC FILE COPY

APPROVED FOR PUBLIC RELEASE; DISTRIBUTION UNLIMITED

86 11 19 058

#### DISCLAIMER

The findings in this report are not to be construed as an official Department of the Army position unless so designated by other authorized documents.

The use of trade name(s) and/or manufacturer(s) does not constitute an official indorsement or approval.

#### DESTRUCTION NOTICE

For classified documents, follow the procedures in DoD 5200.22-M, Industrial Security Manual, Section II-19 or DoD 5200.1-R, Information Security Program Regulation, Chapter IX.

For unclassified, limited documents, destroy by any method that will prevent disclosure of contents or reconstruction of the document.

For unclassified, unlimited documents, destroy when the report is no longer needed. Do not return it to the originator.

REPORT DOCUMENTATION PAGE		READ INSTRUCTIONS BEFORE COMPLETING FORM
1. REPORT NUMBER ARCCB-TR-86034	2. GOVT ACCESSION NO. <b>AD-A174127</b>	3. RECIPIENT'S CATALOG NUMBER
4. TITLE (and Subtitle) ACOUSTOELASTIC EFFECTS IN AUTOFRETTAGED STEEL CYLINDERS		5. TYPE OF REPORT & PERIOD COVERED Final
		6. PERFORMING ORG. REPORT NUMBER
7. AUTHOR(s) W. Scholz and J. Frankel (see reverse)		8. CONTRACT OR GRANT NUMBER(s)
9. PERFORMING ORGANIZATION NAME AND ADDRESS US Army Armament Research, Develop, & Engr Ctr Benet Weapons Laboratory, SMCAR-CCB-TL Watervliet, NY 12189-4050		10. PROGRAM ELEMENT, PROJECT, TASK AREA & WORK UNIT NUMBERS AMCMS No. 6111.01.91A0.011 PRON No. 1A52F59W1A1A
11. CONTROLLING OFFICE NAME AND ADDRESS US Army Armament Research, Develop, & Engr Ctr Close Combat Armaments Center Dover, NJ 07801-5001		12. REPORT DATE October 1986
		13. NUMBER OF PAGES 15
14. MONITORING AGENCY NAME & ADDRESS (if different from Controlling Office)		15. SECURITY CLASS. (of this report)  UNCLASSIFIED
		15a. DECLASSIFICATION/DOWNGRADING SCHEDULE
16. DISTRIBUTION STATEMENT (of this Report)  Approved for public release; distribution unlimited.		
17. DISTRIBUTION STATEMENT (of the abstract entered in Block 20, if different from Report)		
18. SUPPLEMENTARY NOTES  Presented at Ultrasonics International 1985, Kings College, London, Great Britain, 2-4 July 1985. Published in Proceedings of the Conference.		
19. KEY WORDS (Continue on reverse side if necessary and identify by block number) Ultrasonics Residual Stress Acoustoelasticity Steel Third Order Elastic Constants		
20. ABSTRACT (Continue on reverse side if necessary and identify by block number) Residual stresses in short cylinder sections cut from autofrettaged larger steel tubes have been measured by means of the acoustoelastic effect. Ultra- sonic shear waves polarized along the hoop and radial direction and propagating in the axial direction, as well as longitudinal waves, were used. Calibration specimens cut from similar type material were used to determine the velocity changes of longitudinal and shear waves propagating perpendicular to an applied (CONT'D ON REVERSE)		

7. AUHTORS (CONT'D)

W. Scholz  
Department of Physics  
State University of New York at Albany  
Albany, NY 12222

and

US Army Armament Research, Development, and Engineering Center  
Close Combat Armaments Center  
Benet Weapons Laboratory  
Watervliet, NY 12189-4050

20. ABSTRACT (CONT'D)

stress. Third order elastic constants were derived from these measurements. Velocity measurements for zero applied stress along different axes of the cube-shaped calibration specimens indicate the presence of orthorhombic texture. Stress distributions and texture dependent effects within the cylinders have been determined.

UNCLASSIFIED

## TABLE OF CONTENTS

	<u>Page</u>
INTRODUCTION	1
THEORETICAL CONSIDERATIONS AND RESULTS OF CALIBRATION MEASUREMENTS	2
Theoretical Stress Distributions	2
Stress-Velocity Relations	3
Sound Velocities in Cubic-Structure Materials With Texture	5
RESULTS FOR AUTOFRETTAGED CYLINDERS	7
Experimental Details	7
Determination of Texture and Stress From Experimental Velocity Distributions	8
CONCLUSION	10
REFERENCES	12

## TABLES

1. ELASTIC CONSTANTS  $\rho_0 v_1^2$  IN UNITS OF  $10^5$  BAR 7

## LIST OF ILLUSTRATIONS

1. Relative velocity change for shear and longitudinal waves and hoop stress in an 80 percent autofrettaged cylinder. 13
2. Relative velocity change for shear and longitudinal waves and hoop stress in a 100 percent autofrettaged cylinder. 14



Dist Special

A-1

## INTRODUCTION

Ultrasonic velocity measurements are commonly used to determine stresses in materials. Determination of the stresses from the sound velocities generally requires knowledge of the second order or Lamé constants and third order elastic constants (refs 1-3) introduced by Murnaghan (ref 4) in his treatment of finite deformations.

Stresses are often introduced into materials by processes such as autofrettage or thermal quenching. The materials in question, however, may also have been subject to other treatments such as cold rolling or forging. These latter processes are known to introduce so-called "texture effects," i.e., anisotropic orientations in polycrystalline materials. Texture effects can have a profound influence on ultrasonic velocities. Conversely, information on the crystalline orientation distribution function can be derived from ultrasonic velocity measurements (refs 5,6).

This report deals with elastic and texture properties of autofrettaged cylinders made from ASTM A723 steel. Autofrettage is a process in which a hollow cylinder is deformed into the plastic region by application of internal pressure. Releasing the pressure establishes compressive and tensile hoop stresses near the inner and outer diameter of the cylinder, respectively. Compressive radial stresses also result inside the cylinder. In addition, texture can be present within the cylinder due to rotary forging before the application of autofrettage.

---

References are listed at the end of this report.

The specimens used in this work were short circular cylinder sections cut from long autofrettaged tubes which had undergone different amounts of plastic deformation. Ultrasonic velocity measurements were made for shear waves polarized along the hoop and the radial direction and propagating in the axial direction. Longitudinal waves propagating along the axial direction were also used.

For calibration purposes, two auxiliary types of experiments were performed on rectangular prisms cut from the cylinders. First, stress-velocity relations were determined from ultrasonic velocity measurements for transverse and longitudinal waves propagating perpendicular to an externally applied stress. The third order elastic constants  $l$ ,  $m$ , and  $n$  were also determined from these experiments. Second, texture effects were investigated by performing velocity measurements for the nine combinations of the propagation direction (axial, hoop, and radial) and the type of ultrasonic wave (longitudinal and the two polarization directions of the transverse wave).

## THEORETICAL CONSIDERATIONS AND RESULTS OF CALIBRATION MEASUREMENTS

### Theoretical Stress Distributions

Assuming the conditions of plane strain, incompressibility, and ideal plastic behavior together with the von Mises' yield criterion, the residual hoop, radial, and axial stresses  $\sigma_\theta$ ,  $\sigma_r$ , and  $\sigma_z$  in a circular cylinder can be written in closed form as functions of the radial coordinate (ref 7). The solutions fulfill the boundary conditions

$$\sigma_r(a) = \sigma_r(b) = 0 \quad (1)$$

and

$$\int_a^b \sigma_\theta dr = 0 \quad , \quad (2)$$

where a and b are the inner and outer radius, respectively, and the equilibrium condition

$$\sigma_\theta = \sigma_r + r \frac{d\sigma_r}{dr} \quad (3)$$

Predicted hoop stresses are compressive and tensile at the inner and outer diameter, respectively. Predicted radial stresses are always compressive and typically one order of magnitude smaller than the largest hoop stresses. Axial stress is given by one-half the sum of hoop and radial stress. However, cutting short cylinder sections from longer tubes, as done in the present experiment, is expected to relieve the stresses along the axial direction.

#### Stress-Velocity Relations

Relations between ultrasonic velocities and residual stresses can be obtained from the theory of finite deformations. The analysis superimposes an infinitesimal deformation, represented by the ultrasonic wave, on a finite static deformation due to the residual stress. The stress-velocity relations are expressed in terms of the Lamé or second order elastic constants  $\lambda$  and  $\mu$ , and the third order or Murnaghan constants  $k$ ,  $m$ , and  $n$ . The expressions for the stress-strain tensor from which the stress-velocity relations for the general case of triaxial stress can be derived have been given by Hughes and Kelly (ref 1). Explicit expressions for the velocity relations in the case of uniaxial stress can also be found in their study.



The velocity change  $\Delta v_{12}$  of a shear wave, propagating in an isotropic medium along the 1-axis and polarized in a direction perpendicular to it (arbitrarily chosen as the 2-axis) is given in terms of the aforementioned elastic constants and the finite stresses  $\sigma_i$  along the three principal axes as follows (ref 3):

$$\frac{\Delta v_{12}}{v_{0s}} = \frac{1}{6\mu K_0} \left[ (3\lambda + 2\mu)\sigma_1 + (3\lambda + 2\mu + \frac{3n\lambda}{4\mu} + \frac{n}{2})(\sigma_1 + \sigma_2) + (m - \frac{n}{2} - 2\lambda - \frac{n\lambda}{2\mu})(\sigma_1 + \sigma_2 + \sigma_3) \right], \quad (4)$$

where  $K_0 = \lambda + 2\mu/3$  and  $v_{0s}$  is the velocity in the absence of finite stresses. For the longitudinal wave propagating along the 1-axis one finds similarly, setting  $v_{0l}$  equal to the longitudinal wave velocity in the absence of stress

$$\frac{\Delta v_{11}}{v_{0l}} = \frac{1}{4\mu(\lambda + 2\mu)} (4\lambda + 4m + 10\mu)\sigma_1 + \frac{1}{6K_0(\lambda + 2\mu)} (2\lambda - 4\lambda - \frac{2m\lambda}{\mu} - \frac{2\lambda^2}{\mu})(\sigma_1 + \sigma_2 + \sigma_3) \quad (5)$$

The coefficients multiplying the stresses in Eqs. (4) and (5) were determined from measurements of velocity changes of ultrasonic waves propagating through rectangular test bars with cross-sectional area 1/2 by 1/2-inch, perpendicular to the direction of applied tensile stress ( $\sigma_1 = 0$ ). The test bars were cut from autofrettaged cylinders with the long dimension (the direction of applied stress) along the hoop direction. Partial results of these measurements have been reported previously (ref 3). For shear waves we obtained for the case where the polarization is parallel to the stress

$$(\Delta v_{12}/v_{0s}) = (-7.80 \pm 0.30) \times 10^{-2} \sigma_2 [10^5 \text{ bar}] \quad (6)$$

and for polarization perpendicular to the stress

$$(\Delta v_{12}/v_{0s}) = (0.57 \pm 0.10) \times 10^{-2} \sigma_3 [10^5 \text{ bar}] \quad . \quad (7)$$

For longitudinal waves we measured

$$(\Delta v_{11}/v_{0l}) = (0.76 \pm 0.10) \times 10^{-2} \sigma_{2,3} [10^5 \text{ bar}] \quad . \quad (8)$$

Using the results of Eqs. (6) through (8) and the values of the Lamé constants  $\lambda$  and  $\mu$ , which will be discussed in the next section, Eqs. (4) and (5) can be solved for the Murnaghan constants. Values obtained are  $l = -38.8 \pm 3.6$ ,  $m = -62.4 \pm 2.4$ , and  $n = -74.7 \pm 1.6$ , in units of  $10^5 \text{ bar}$ .

The values of the elastic constants determined above in conjunction with Eqs. (4) and (5), can be used to predict velocity changes due to stresses along the direction of propagation. One obtains for shear waves

$$(\Delta v_{12}/v_{0s}) = (-1.54 \pm 0.30) \times 10^{-2} \sigma_1 [10^5 \text{ bar}] \quad (9)$$

and for longitudinal waves

$$(\Delta v_{11}/v_{0l}) = (-14.5 \pm 1.1) \times 10^{-2} \sigma_1 [10^5 \text{ bar}] \quad . \quad (10)$$

It is worth noting that longitudinal waves are about ten times more sensitive to residual stresses along the direction of propagation than shear waves. The acoustoelastic constants in Eqs. (6) through (10) and the values of the Murnaghan constants given above are in reasonable agreement with values reported by other investigators for somewhat different types of steel (refs 8,9).

#### Sound Velocities in Cubic-Structure Materials With Texture

Rolling or forging of polycrystalline materials can introduce partial alignment of the individual single crystals, so-called texture, which causes a dependence of the ultrasonic velocities on the propagation and polarization direction. In the most general case, the material develops orthorhombic

texture, corresponding to three orthogonal planes of symmetry. A less complicated case is fiber texture which corresponds to a medium which is elastically insensitive to rotation about one axis. From symmetry considerations, one would argue that this axis should coincide with the direction of the striking force during forging.

The ultrasonic velocities  $v_{ij}$ , where  $i$  refers to the propagation and  $j$  to the polarization direction, are given as (refs 5,6):

$$\rho_0 v_{11}^2 = \lambda + 2\mu + 2ct_{11} \quad (11)$$

and

$$\rho_0 v_{1j}^2 = \mu + ct_{1j} \quad (12)$$

where  $c = c_{11} - c_{12} - 2c_{44}$  in terms of the elastic constants of the cubic single crystal. Expressions for the texture factors  $t_{ij}$  are also given in References 5 and 6. It is worth noting that  $t_{ij} = t_{ji}$  and that

$$\sum_j \rho_0 v_{1j}^2 = \lambda + 4\mu \quad (13)$$

which is independent of texture.

Measurements were performed on a rectangular prism with dimensions 1/2 by 1/2 by 5/8-inch cut from an autofrettaged tube with its surfaces parallel to the axial, hoop, and radial direction which will be labeled 1, 2, and 3, respectively. Velocity measurements were performed with the pulse-echo overlap technique. Ten and fifteen MHz longitudinal and five and fifteen MHz shear transducers were used in order to arrive at an unambiguous identification of the correct pulse overlap (ref 10). Table 1 lists the corresponding elastic constants  $\rho_0 v^2$  ( $\rho_0 = 7.84 \times 10^3 \text{ kg/m}^3$ ) along with the sums of Eq. (13). The results indicate that Eq. (13) is fulfilled to a high degree of accuracy.

TABLE 1. ELASTIC CONSTANTS  $\rho_0 v_{ij}^2$  IN UNITS OF  $10^5$  BAR

	i=1	i=2	i=3	$\sum_i$
j = 1	27.0170	7.9591	8.0176	42.9937
j = 2	7.9541	27.0289	7.9971	42.9801
j = 3	8.0151	7.9921	26.9728	42.9800
$\sum_j$	42.9862	42.9801	42.9875	

The data in Table 1 indicate the presence of texture; furthermore, to first order, it appears to be fiber texture. In the case of fiber texture where there is one elastic axis, the two longitudinal waves propagating perpendicular to it are equal in velocity. Of the transverse waves, the two polarized and propagating perpendicular to the elastic axis are equal and differ from the remaining four which are in turn equal to each other. The fact that this last condition is violated to some degree indicates that the texture is more precisely characterized as orthorhombic.

By forming averages of the values in Table 1, we derive  $\lambda = 11.03 \times 10^5$  bar and  $\mu = 7.99 \times 10^5$  bar for the Lamé constants in this particular specimen.

#### RESULTS FOR AUTOFRETTAGED CYLINDERS

##### Experimental Details

The specimens for these experiments were right circular cylinders, one to two inches in height, with inner radius  $a$  and outer radius  $b$  of approximately three and six inches, respectively, which had been cut from longer

autofrettaged tubes. Velocity changes were determined by measuring the change in return time of one echo (typically the fifth) with respect to a reference time which was chosen as the return time near the outer diameter for the shear wave polarized in the hoop direction (ref 3). Return times for the radially polarized wave were determined by rotating the transducer. A separate reference, also near the outer diameter, was used for longitudinal waves. Standard commercial transducers were used in these experiments. The time resolution of the experiment was better than 5 ns, thus relative velocity changes were determined to better than one part in  $10^4$ .

#### Determination of Texture and Stress From Experimental Velocity Distributions

Figures 1 and 2 show the observed velocity changes for the longitudinal (full diamonds) and the two transverse waves (full circles and squares for polarization in the hoop and radial direction, respectively) with radial distance, plotted vs.  $(r-a)/(b-a)$ . Some qualitative features are immediately obvious. First, the shear wave polarized along the hoop direction exhibits large velocity changes with radial position. If we establish a base line for the velocity in the zero stress state using the boundary condition Eq. (2), and the proportionality between stress and relative velocity change, the measurements indicate compressive and tensile hoop stresses near the inner and outer diameter, respectively. Second, the shear wave polarized along the radial direction is displaced toward larger velocities from the base line established above. In view of the boundary conditions (Eq. (1)), this cannot be due to radial stresses. The direction and magnitude of the displacement is approximately the same as for the calibration specimen of Table 1 and

therefore can be explained by a texture effect. Third, velocity changes for the longitudinal wave are comparatively small. In addition, since the acoustoelastic coefficient in Eq. (10) is rather large, it follows that residual longitudinal stresses are small as expected and can be neglected in the analysis of the transverse wave velocities.

The major contribution to the observed texture effect appears to be independent of the radial position and thus does not influence the analysis for hoop stresses in which the zero-stress base line is established through application of the boundary condition Eq. (2). However, radius dependent texture effects are clearly present, most notably in Figure 1, which shows an oscillatory behavior in the velocity of the transverse wave polarized along the radial direction. This is at variance with expected radial stress distributions and the equilibrium condition Eq. (3) and must, therefore, be due to texture.

For the idealized situation of fiber texture with an elastic axis along the radial direction, theory predicts (refs 5,6) the texture factors in Eqs. (11) and (12) to be in a ratio of  $t_{zr}:t_{z\theta}:2t_{zz} = -4:1:3$ . That is, texture induced velocity changes will be most pronounced for the radially polarized shear wave and of lesser magnitude and opposite sign for the transverse wave polarized along the hoop direction and the longitudinal wave. This is indeed more or less the observed behavior for the oscillatory structure in Figure 1.

In view of the discussion above and since hoop stresses are expected to be typically one order of magnitude larger than radial stresses,  $\Delta v_{z\theta}/v_{0\theta}$  primarily reflects the stress distribution. The lefthand scales in Figures 1

and 2 for the hoop stress are drawn using the acoustoelastic constant of Eq. (6). Radial stresses, in addition to being small, enter through the small coefficient of Eq. (7) and can be neglected. The curves are drawn for 80 and 100 percent autofrettage, respectively, using a yield strength  $\sigma_0 = 0.12 \times 10^5$  bar (174 Ksi).

The open symbols in Figures 1 and 2 are obtained by subtracting from the measured velocity distributions the calculated contributions due to theoretical hoop and radial stresses. They reflect primarily the radial dependence of the texture factors which are expected to be of opposite sign for the radially polarized shear wave and the longitudinal wave. For fiber texture, the apparent variations in the relative velocity change are expected to be reduced by a factor  $(3/4)(v_{0s}/v_{0l})^2 = 0.22$  for the longitudinal wave as compared to the radially polarized shear wave. The variations in Figures 1 and 2 are reasonably consistent with this expectation. Thus, one might conclude that the velocity changes observed for the longitudinal wave also reflect texture and that residual stresses are indeed essentially zero as expected.

## CONCLUSION

Velocity changes of shear and longitudinal waves propagating along the axis of short autofrettaged ASTM A723 steel cylinders can be used to derive information on residual stresses and texture effects. The shear wave polarized in the hoop direction shows little texture effect and can be used to yield information on the hoop stress distribution via the acoustoelastic effect. The shear wave polarized in the radial direction primarily reflects

variations of the texture factor with radial position, as does the longitudinal wave. Residual radial and longitudinal stresses are difficult to separate from texture effects, but longitudinal wave measurements are consistent with zero axial residual stress. Theoretical stress distributions can give a reasonable account of the measured hoop stresses.



## REFERENCES

1. D. S. Hughes and J. L. Kelly, Phys. Rev., Vol. 92, 1953, p. 1145.
2. F. Bach and V. Askegaard, "General Stress-Velocity Expressions in Acoustoelasticity," Exp. Mech., Vol. 19, No. 2, February 1979, p. 69.
3. J. Frankel, W. Scholz, G. Capsimalis, and W. Korman, "Residual Stress Measurement in Circular Steel Cylinders," 1983 Ultrasonics Symposium Proceedings, (B. R. McAvoy, ed.), IEEE, New York, Vol. 2, 1983, pp. 1009-1012.
4. P. D. Murnaghan, Finite Deformation of an Elastic Solid, Wiley, New York, 1951 (reprinted by Dover Publications, New York, 1967).
5. C. M. Sayers, "Ultrasonic Velocities in Anisotropic Polycrystalline Aggregates," J. Phys. D., Vol. 15, No. 11, November 1982, pp. 2157-2167.
6. E. Schneider, S. L. Chu, and K. Salama, "Influence of Texture on the Temperature Dependence of Ultrasonic Velocities," 1984 Ultrasonics Symposium Proceedings, (B. R. McAvoy, ed.), IEEE, New York, Vol. 2, 1984, pp. 944-949.
7. W. Prager and P. G. Hodge, Theory of Perfectly Plastic Solids, Dover Publications, New York, 1950.
8. D. M. Egle and D. E. Bray, "Measurement of Acoustoelastic and Third-Order Elastic Constants For Rail Steel," J. Acoust. Soc. Am., Vol. 60, No. 3, September 1976, pp. 741-744.
9. G. Mott and M. C. Tsao, "Acousto-Elastic Effects in Two Structural Steels," in Nondestructive Methods for Material Property Determination, (C. O. Ruud and R. E. Green, Jr., eds.) Plenum, New York, 1984, p. 377.
10. W. Scholz and J. Frankel, to be published.

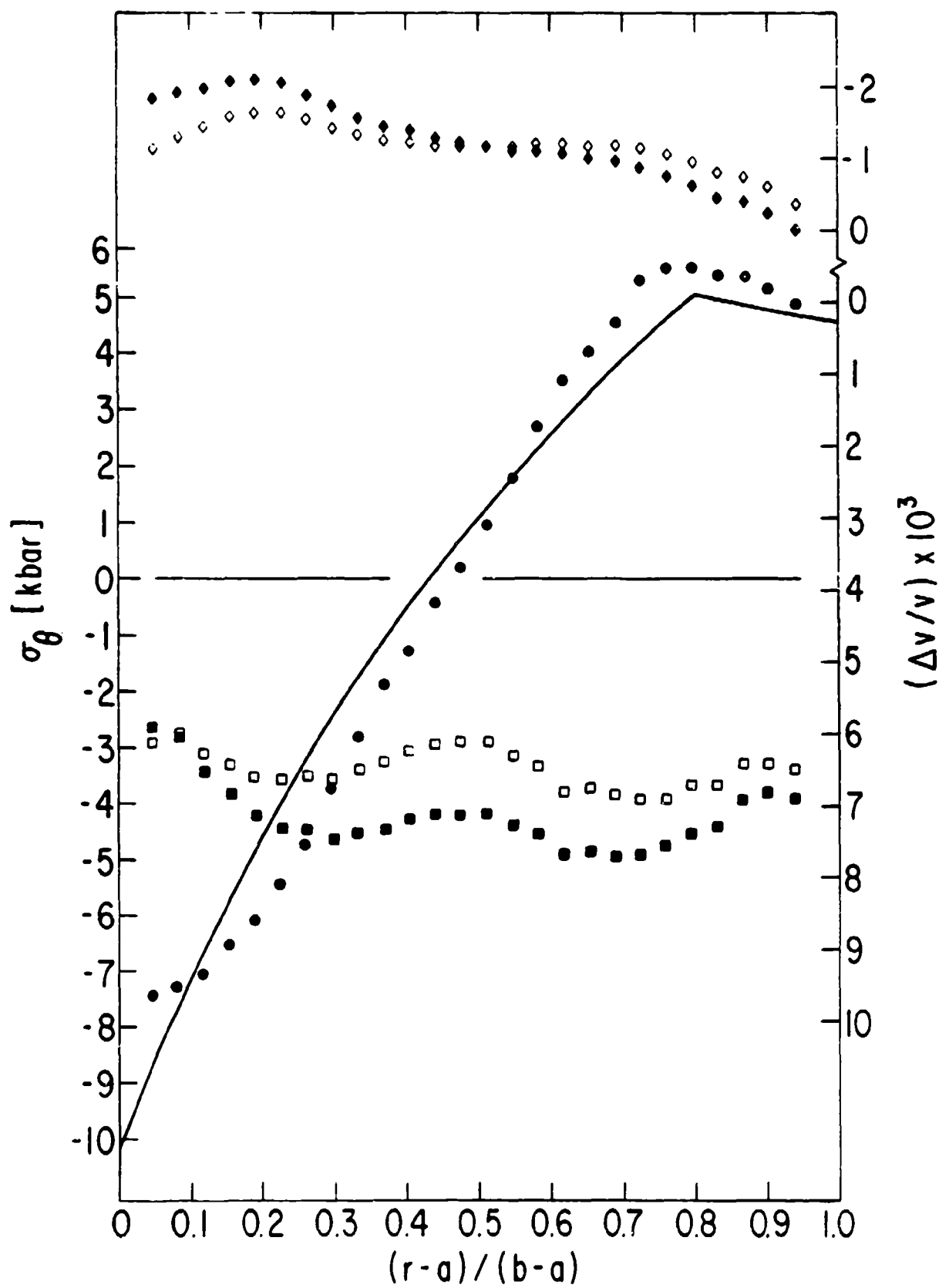


Figure 1. Relative velocity change for shear and longitudinal waves and hoop stress in an 80 percent autofrettaged cylinder.

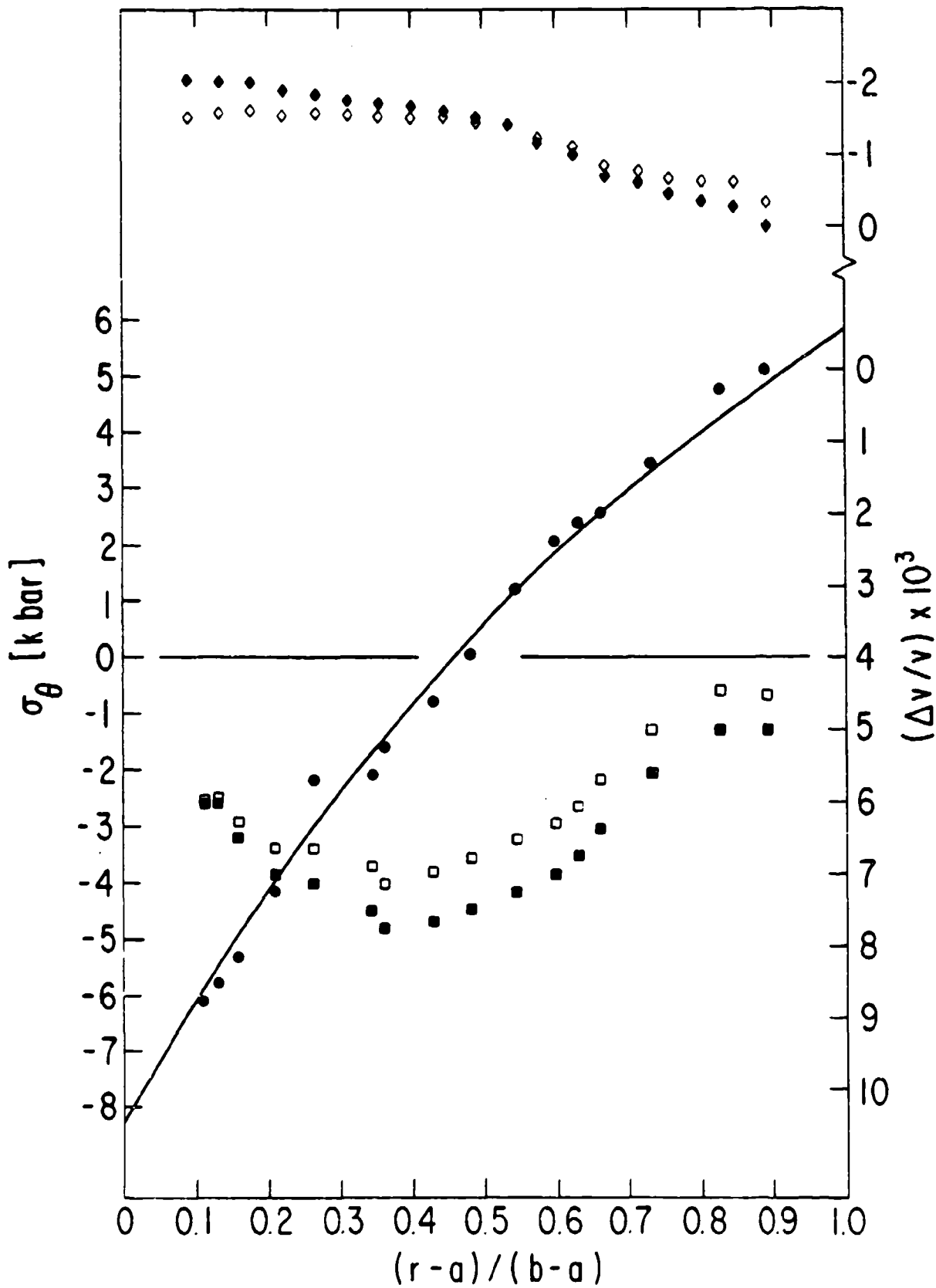


Figure 2. Relative velocity change for shear and longitudinal waves and hoop stress in a 100 percent autofrettaged cylinder.

# TECHNICAL REPORT INTERNAL DISTRIBUTION LIST

	<u>NO. OF COPIES</u>
CHIEF, DEVELOPMENT ENGINEERING BRANCH	
ATTN: SMCAR-CCB-D	1
-DA	1
-DP	1
-DR	1
-DS (SYSTEMS)	1
-DC	1
-DM	1
CHIEF, ENGINEERING SUPPORT BRANCH	
ATTN: SMCAR-CCB-S	1
-SE	1
CHIEF, RESEARCH BRANCH	
ATTN: SMCAR-CCB-R	2
-R (ELLEN FOGARTY)	1
-RA	1
-RM	1
-RP	1
-RT	1
TECHNICAL LIBRARY	5
ATTN: SMCAR-CCB-TL	
TECHNICAL PUBLICATIONS & EDITING UNIT	2
ATTN: SMCAR-CCB-TL	
DIRECTOR, OPERATIONS DIRECTORATE	1
DIRECTOR, PROCUREMENT DIRECTORATE	1
DIRECTOR, PRODUCT ASSURANCE DIRECTORATE	1

NOTE: PLEASE NOTIFY DIRECTOR, BENET WEAPONS LABORATORY, ATTN: SMCAR-CCB-TL,  
OF ANY ADDRESS CHANGES.

# TECHNICAL REPORT EXTERNAL DISTRIBUTION LIST

	<u>NO. OF COPIES</u>		<u>NO. OF COPIES</u>
ASST SEC OF THE ARMY RESEARCH & DEVELOPMENT ATTN: DEP FOR SCI & TECH THE PENTAGON WASHINGTON, D.C. 20315	1	COMMANDER US ARMY AMCCOM ATTN: SMCAR-ESP-L ROCK ISLAND, IL 61299	1
COMMANDER DEFENSE TECHNICAL INFO CENTER ATTN: DTIC-DDA CAMERON STATION ALEXANDRIA, VA 22314	12	COMMANDER ROCK ISLAND ARSENAL ATTN: SMCRI-ENM (MAT SCI DIV) ROCK ISLAND, IL 61299	1
COMMANDER US ARMY MAT DEV & READ COMD ATTN: DRCD-EG 5001 EISENHOWER AVE ALEXANDRIA, VA 22333	1	DIRECTOR US ARMY INDUSTRIAL BASE ENG ACTV ATTN: DRXIB-M ROCK ISLAND, IL 61299	1
COMMANDER ARMAMENT RES & DEV CTR US ARMY AMCCOM ATTN: SMCAR-FS	1	COMMANDER US ARMY TANK-AUTMV R&D COMD ATTN: TECH LIB - DRSTA-TSL WARREN, MI 48090	1
SMCAR-FSA	1	COMMANDER US ARMY TANK-AUTMV COMD ATTN: DRSTA-RC WARREN, MI 48090	1
SMCAR-FSM	1		
SMCAR-FSS	1		
SMCAR-AEE	1		
SMCAR-AES	1		
SMCAR-AET-O (PLASTECH)	1		
SMCAR-MSI (STINFO)	2		
DOVER, NJ 07801			
DIRECTOR BALLISTICS RESEARCH LABORATORY ATTN: AMXBR-TSB-S (STINFO) ABERDEEN PROVING GROUND, MD 21005	1	US ARMY MISSILE COMD REDSTONE SCIENTIFIC INFO CTR ATTN: DOCUMENTS SECT, BLDG. 4484 REDSTONE ARSENAL, AL 35898	2
MATERIEL SYSTEMS ANALYSIS ACTV ATTN: DRXSY-MP ABERDEEN PROVING GROUND, MD 21005	1	COMMANDER US ARMY FGM SCIENCE & TECH CTR ATTN: DRXST-SD 220 7TH STREET, N.E. CHARLOTTESVILLE, VA 22901	1

**NOTE:** PLEASE NOTIFY COMMANDER, ARMAMENT RESEARCH, DEVELOPMENT, AND ENGINEERING CENTER, US ARMY AMCCOM, ATTN: BENET WEAPONS LABORATORY, SMCAR-CCB-TL, WATERVLIET, NY 12189-4050, OF ANY ADDRESS CHANGES.

# TECHNICAL REPORT EXTERNAL DISTRIBUTION LIST (CONT'D)

	NO. OF COPIES		NO. OF COPIES
COMMANDER US ARMY LABCOM MATERIALS TECHNOLOGY LAB ATTN: SLCMT-IML WATERTOWN, MA 01272	2	DIRECTOR US NAVAL RESEARCH LAB ATTN: DIR, MECH DIV CODE 26-27, (DOC LIB) WASHINGTON, D.C. 20375	1 1
COMMANDER US ARMY RESEARCH OFFICE ATTN: CHIEF, IPO P.O. BOX 12211 RESEARCH TRIANGLE PARK, NC 27709	1	COMMANDER AIR FORCE ARMAMENT LABORATORY ATTN: AFATL/MN AFATL/MNG EGLIN AFB, FL 32542-5000	1 1
COMMANDER US ARMY HARRY DIAMOND LAB ATTN: TECH LIB 2800 POWDER MILL ROAD ADELPHIA, MD 20783	1	METALS & CERAMICS INFO CTR BATTELLE COLUMBUS LAB 505 KING AVENUE COLUMBUS, OH 43201	1
COMMANDER NAVAL SURFACE WEAPONS CTR ATTN: TECHNICAL LIBRARY CODE X212 DAHLGREN, VA 22448	1		

**NOTE:** PLEASE NOTIFY COMMANDER, ARMAMENT RESEARCH, DEVELOPMENT, AND ENGINEERING CENTER, US ARMY AMCCOM, ATTN: BENET WEAPONS LABORATORY, SMCAR-CCB-TL, WATERVLIET, NY 12189-4050, OF ANY ADDRESS CHANGES.